

A non-intrusive reduced order model for light water reactor core stability analysis

*Original*

A non-intrusive reduced order model for light water reactor core stability analysis / Abrate, N., Dulla, S., Pedroni, N.. - ELETTRONICO. - (2020), pp. 4946-4952. (30th European Safety and Reliability Conference, ESREL 2020 and 15th Probabilistic Safety Assessment and Management Conference, PSAM 2020 Venice (Italy) 2020).

*Availability:*

This version is available at: 11583/2962357 since: 2022-05-01T17:59:32Z

*Publisher:*

Research Publishing Services

*Published*

DOI:

*Terms of use:*

This article is made available under terms and conditions as specified in the corresponding bibliographic description in the repository

*Publisher copyright*

(Article begins on next page)

# A Non-Intrusive Reduced Order Model for Light Water Reactor core stability analysis

Nicolò Abrate, Sandra Dulla, Nicola Pedroni

*NEMO Group, ENERGY Department, Politecnico di Torino, Italy. E-mail: nicolo.abrate@polito.it, sandra.dulla@polito.it, nicola.pedroni@polito.it*

A non-intrusive reduced order model for studying the nuclear reactor core stability in presence of localised perturbations due to operational uncertainties is analysed. Following the standard neutronics calculation chain, a two-step model based on a combination of POD and RBF approaches is proposed in order to reduce the computational time of both the cell calculation, devoted to produce homogenised data for the full-core diffusion calculation, and the diffusion calculation itself. The results presented suggest that, while the cell model seems adequate to reproduce untrained operating conditions, the diffusion model still needs to be properly tuned, improving the training set quality.

**Keywords:** Light Water Reactors, physical perturbation, stability analysis, Smolyak grid, Radial Basis Function, Proper Orthogonal Decomposition

## 1. Introduction

In order to comply with more and more strict safety, environmental and cost requirements, Generation-III+ Pressurized Water Reactors (PWRs) have new design features aiming at extending the life of the plant, reducing the radioactive waste and incorporating passive safety principles. In particular, as far as the neutronic design is concerned, the core is endowed with a "heavy", stainless-steel reflector that, compared to a traditional "light", water reflector, minimizes the neutrons leakage, reducing the radiological risk and increasing the overall energy production (Sargeni et al., 2016). Nevertheless, the adoption of such a reflector poses some serious stability issues, since the neutron distribution inside the core is more sensitive to localised perturbations that can be induced by fuel assemblies fabrication tolerance, pump operational uncertainties and other local disturbances. Due to the random nature of such phenomena, they basically can compensate each other or can superimpose. In the latter situation, the worst-case scenario (Sargeni et al., 2016) is the occurrence of the flux *tilt*, i.e. a strong neutron flux spatial distortion that translates into a power disequilibrium. Flux tilting is especially dangerous during the start-up phase (Hot Zero Power, HZP), when the thermal feedback mechanisms are not yet effective in damping such flux spatial instabilities (Sargeni et al., 2016) and the core instrumentation is not able to detect tilt due to the very low power level.

Therefore, a thorough sensitivity study of the tilt phenomenon via numerical simulation is required in order to assess the core safety. The approach traditionally employed for the characterisation of the system spatial effects is the Gen-

eralised Perturbation Technique (GPT), which is very popular in reactor physics applications because it allows to reduce considerably the computational burden associated to the flux calculations by means of the evaluation of the higher-order modes of the multi-group neutron diffusion equation and its adjoint on the unperturbed core and in their use as an expansion basis for the flux on the perturbed core (Gandini, 1987). In spite of its popularity, this approach may have some convergence issues if the perturbed regions in the system are too large or if the perturbation intensity is too strong (Abrate et al., 2019).

An alternative to tackle the huge computational cost required for the tilt characterisation consists in the adoption of a Parametrised Non-Intrusive Reduced Order Model (P-NIROM), similar to the one recently developed for fluid-dynamics applications (Xiao et al., 2017). This kind of reduced order model allows to split the calculation in an off-line part, where the meta-model is trained over a set of high fidelity simulations, evaluated on a set of parameters, and in an on-line part, where an approximated solution over untrained parameters is obtained with a limited computational cost. While GPT requires the calculation of an *a priori* fixed number of flux and flux-adjoint harmonics, P-NIROM allows to define an adaptive simulation strategy, since the number of calculations in the training phase could be modulated according to the required tolerance in each parameters space region. Moreover, due to its non-intrusiveness, the algorithm is fully compatible with the already validated codes employed for the reactors licensing, as it does not require any code modifications, treating it as a black-box.

The main purpose of this contribution is thus

to present the preliminary development and results of an *ad hoc* Neutronics Parametrised Non-Intrusive Reduced Order Model (NP-NIROM) for the characterisation of nuclear reactor spatial effects.

In section 2 we present the physico-mathematical model typically solved in the neutronics framework, while in section 3 we propose the two-step reduced order model for this neutronics application. Finally, in section 4 some preliminary results are shown and in section 5 some conclusions are drawn.

## 2. Physico-mathematical model

The reference physical model employed to study the steady state neutron distribution in the 6-dimensional phase space (space, energy and flying direction) is the Boltzmann linear transport equation (Wigner and Weinberg, 1958). The numerical solution of such equation on the whole core, whether via detailed Monte Carlo simulations or approximated deterministic schemes, often provides unnecessary detail and is extremely computationally intensive, therefore a typical neutronic calculation for a standard reactor mainly consists of two steps (Henry, 1975),

- (1) an accurate transport calculation over the main reactors regions in order to retrieve spatially homogenised and energy condensed material data at the assembly level (cell calculation),
- (2) a few-energy groups diffusion calculation at the full-core level with the diffusion coefficient and macroscopic cross sections produced in the cell calculation (full-core calculation).

The two-step nature of the neutronic criticality calculation allows to treat a complex, multi-scale system like a nuclear reactor in a quite simple way, gathering most of the computationally intensive calculations in the first step, where the attention is focused more on the energy and the angular variables than on the space ( $\approx$  thousands of energy groups and hundreds of angular directions for a deterministic calculation, continuous-energy and angle with Monte Carlo approach). After the first step, the obtained collapsed parameters, which are averaged preserving the reaction rates inside the system, can finally be employed for faster space-oriented calculations, which are strictly linked to the power density distribution of the reactor. For the analysis of a typical PWR core, a two-group diffusion model is usually applied as a good compromise between accuracy and computational cost

(Wigner and Weinberg, 1958),

$$\begin{cases} -\nabla \cdot D_1 \nabla \phi_1 + \Sigma_{r,1} \phi_1 - \frac{1}{k_{\text{eff}}} \nu \Sigma_{f,2} \phi_2 = 0 \\ -\nabla \cdot D_2 \nabla \phi_2 + \Sigma_{r,2} \phi_2 - \Sigma_{s,1 \rightarrow 2} \phi_1 = 0, \end{cases} \quad (1)$$

where  $\phi$  is the flux,  $D$  is the diffusion coefficient,  $\Sigma_r$  is the removal cross section,  $\nu \Sigma_f$  is the product between the neutrons emitted by a fission and the fission cross section, and  $\Sigma_{s,1 \rightarrow 2}$  is the slowing down cross section. For easiness of notation, the space dependence of all the previously mentioned variables have been omitted and the fast fission has been assumed negligible. The subscripts 1 and 2 stand for fast ( $>0.625$  eV) and thermal ( $<0.625$  eV) energy groups, respectively. Since the system of Partial Differential Equations (PDEs) is homogeneous, the criticality eigenvalue  $k_{\text{eff}}$  is introduced in front of the production term so to retrieve the non-trivial steady state distribution.

In order to properly characterise the spatial effects induced by physical perturbations inside the core, both the steps should be addressed carefully in the construction of the meta-model, as it will be detailed in the next section.

## 3. Two-step reduced order modelling

As mentioned, usually most of the computational burden associated to a criticality eigenproblem is related to the cell calculation, which is therefore performed only for a limited number of core configurations (e.g. control rods inserted and withdrawn, different operating temperatures...). Once this resource-demanding step is completed, the full-core calculations can be carried out in a shorter but still significant amount of time to verify the criticality condition ( $k_{\text{eff}} = 1$ ), assess the core power distribution, with different fuel loading patterns, and so on. However, in order to have a reliable picture of the overall system response to localised perturbations at the assembly level, the material constants computed in the first step should be evaluated for each perturbation considered. On top of that, different assemblies may be affected by different disturbances in the same configuration, therefore a potentially huge number of cell calculations may be required in order to get a solution training set leading to an acceptable error.

The approach devised to overcome this issue mimics the two-step criticality methodology, relying on two independent P-NIROMs for each criticality step.

### 3.1. Cell meta-model

The first P-NIROM method takes as input the main parameters of the cell and computes a surrogate set of condensed data. The implementation details of the model are presented in the following.

### 3.1.1. Parameter space sampling

For an efficient mapping of the parameter space  $\mathbb{R}^p$ , where  $p$  is the number of parameters, the Smolyak algorithm has been employed (Smolyak, 1963). This technique, originally conceived for interpolating high-dimensional functions with a few points on hypercubes, allows to select the most important points from the tensor products of an unidimensional grid. The latter is usually built using nested sets of points, like, for example, some subsets of Chebyshev polynomials extrema.

While the tensor products suffers from the curse of dimensionality, i.e. the set of points grows exponentially with respect to  $p$ , the Smolyak grid dimension scales like a polynomial depending both on  $p$  and on the grid approximation level  $\mu$ , which is a free parameter related to the number of points in the sparse grid.

Since the points used to generate the grid are nested, one can choose an arbitrarily low grid approximation level  $\mu$  for the parameter space and then increase *a posteriori* the number of training points, reusing the already existing simulations. On top of that, in case some specific dimension in  $\mathbb{R}^p$  requires a higher accuracy, an anisotropic Smolyak grid could be assembled, increasing the flexibility of the training point selection procedure (Judd et al., 2014).

### 3.1.2. Model training

Once the computationally intensive phase is concluded, the Proper Orthogonal Decomposition (POD) is adopted to reduce the training set dimensionality approximating the parametric snapshots, i.e. the set of material constants retrieved from the complete cell calculation, with an expansion on a set of  $t$  representative basis functions  $\vec{\psi}$ ,

$$\vec{y}_j = \sum_{i=1}^t a_{i,j} \vec{\psi}_i \quad j = 0, \dots, n, \quad (2)$$

where  $a_{i,j}$  is the weighting coefficient associated to the  $i$ -th basis function to approximate the  $j$ -th snapshot.

POD is a standard technique to reduce a set of data to its fundamental behaviour (Volkwein, 2013), and can be carried out via Singular Value Decomposition (SVD) or EigenValue Decomposition (EVD). Due to its better numerical stability (Sullivan, 2015), the POD method is performed using the SVD,

$$\hat{Y} = \hat{\Psi} \hat{\Sigma} \hat{\Phi}^T, \quad (3)$$

where  $\hat{Y} = [\vec{y}_1, \vec{y}_2, \dots, \vec{y}_n] \in \mathbb{R}^{m \times n}$  is the snapshot matrix,  $\hat{\Psi} \in \mathbb{R}^{m \times m}$  is the column-wise set of  $\hat{Y}$  left eigenvectors,  $\hat{\Sigma} \in \mathbb{R}^{m \times m}$  contains  $\hat{Y}$  singular values and  $\hat{\Phi} \in \mathbb{R}^{m \times m}$  is the column-wise set of  $\hat{Y}$  right eigenvectors.

Since the  $\hat{Y}$  singular values  $\sigma_i$  are a monotonically decreasing sequence ( $\sigma_1 > \sigma_2 > \dots > \sigma_r$ , where  $r$  is the rank of  $\hat{Y}$ ), and they are proportional to the information carried out by each basis function, it is easy to truncate the POD to a number  $t < r$ , in order to reduce the system dimension. The value of  $t$  is chosen fixing the value of the POD basis energy, i.e. the ratio

$$\mathcal{E}(t) = \frac{\sum_{i=1}^t \sigma_i^2}{\sum_{i=1}^r \sigma_i^2}, \quad (4)$$

equal to a certain value slightly smaller than 1, which is the value for the limit case  $t = r$ .

After the truncated basis  $\hat{\Psi}_t$  calculation, the complete set of weighting coefficients is computed by means of the matrix product (Rogers et al., 2012)

$$\hat{A} = \hat{\Psi}_t^T \hat{Y}, \quad \hat{A} \in \mathbb{R}^{t \times n}. \quad (5)$$

In order to complete the training process, an interpolation method able to approximate the reduced order cell calculation also over untrained points has to be properly defined. In this work, we rely on the Radial Basis Function (RBF) approach, where the interpolation process is carried out again with a linear combination of arbitrarily chosen basis functions  $f$ , whose value depends on the euclidean distance between the untrained parameter set  $\vec{p}_u$  and the training parameter sets  $\vec{p}_i$ ,

$$\vec{a}_u = \sum_{i=1}^n f(\|\vec{p}_i - \vec{p}_u\|) \vec{b}_i, \quad \vec{a}_u \in \mathbb{R}^t. \quad (6)$$

The vector  $\vec{a}_u$ , i.e. the untrained solution on the reduced order space, can be mapped onto the original  $m$ -dimensional space by means of a projection on the truncated POD basis,

$$\vec{y}_u = \hat{\Psi}_t \vec{a}_u. \quad (7)$$

Independently of the kind of function  $f$  chosen, the RBF weighting coefficients matrix  $\hat{B} = [\vec{b}_1, \dots, \vec{b}_n]$  is computed inverting the matrix equation  $\hat{A} = \hat{B} \hat{F}$  obtained from (6), where the columns  $\vec{a}$  of  $\hat{A}$  are the POD coefficients computed with (5), i.e. the reduced order training solutions,

$$\hat{B} = \hat{A} \hat{F}^{-1}, \quad \hat{B} \in \mathbb{R}^{t \times n}, \quad (8)$$

where  $\hat{F} = [\vec{f}_1, \vec{f}_2, \dots, \vec{f}_n]$  is the RBF matrix, whose columns are the  $\vec{f}_i = [f(\|\vec{p}_1 - \vec{p}_i\|), \dots, f(\|\vec{p}_n - \vec{p}_i\|)]$  vectors.

### 3.2. Diffusion meta-model

Also for the diffusion calculation surrogate model, the POD-RBF technique presented in the previous section can be applied, with some precautions related to the problem dimensionality, which is much more significant than for the cell calculation case, and to the fact that the perturbations are spatially distributed. Since the P-NIROM-like models are built for a well-defined parameter sets size  $p$ , dealing with a set of spatially-dependent perturbations with random amplitude and number is not trivial. One could tackle the problem via a spatial decomposition of the input parameters, but for this work we preferred to carry out some preliminary tests fixing both the perturbations number and intensity, in order to focus more on the spatial dependence of the perturbations.

Another relevant aspect to be taken into account dealing with the reduced order modelling of the second step is related to the fact that, in addition to the errors due to the POD truncation and to the RBF interpolation, one should take into account also the error coming from the cell P-NIROM associated to the set of input material parameters in eq. (1). Because of this, for this contribution we have considered stand-alone calculations for the two steps, leaving their coupling and the study of the resulting error as future developments.

### 3.3. Model errors

As mentioned in the previous section, the overall modelling errors can be attributed basically to the truncation of the POD basis and to the RBF interpolation. While the first can be controlled thanks to the Eckart-Young theorem (Sullivan, 2015), which bounds the euclidean norm between the full order solution and the truncated full order solution,

$$\|\vec{y}_{u,r} - \vec{y}_u\| = \|\vec{y}_{u,r} - \hat{\Psi}_t \vec{a}_u\| \leq \sigma_{t+1}, \quad (9)$$

the interpolation error is more difficult to control, due to the so-called RBF uncertainty principle (Schaback, 1995), according to which the choice of the radial basis shape parameter should be a compromise between the function amplitude and  $\hat{F}$  matrix condition number. Moreover, to the authors knowledge, the definition of a suitable *a priori* interpolation error estimator, like eq. (9) for the POD, is not given. Therefore, in this work, we limit ourselves to compare the so-called fill-distance of the training points, i.e.

$$d = \sup(\min(\|\vec{p}_i - \vec{p}_j\|)), \quad \forall \vec{p}_i, \vec{p}_j \in \mathbb{R}^p \quad (10)$$

with the minimum distance between an untrained point and the RBF centers.

## 4. Results

In this section, the main results obtained with the two models are presented. The parameter

space sampling, the POD basis extraction and the RBF interpolation have been carried out with in-house Python 3 modules, while the Monte Carlo code Serpent-2 (Leppänen et al., 2015) has been adopted for the training cell calculations and the open-source finite element code FreeFEM++ has been used for the diffusion calculation (Hecht, 2012).

### 4.1. Case of study

The models have been tested on the UAM (Uncertainty in Analysis Modeling) benchmark, a Gen-III+ like core (Ivanov et al., 2013). The system, which consists of 529 squared assemblies with an edge of 21.61 cm each, is depicted in Figure 1. As

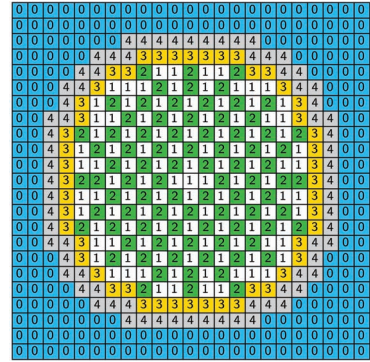


Fig. 1.: 2D representation of the UAM core in its Uranium Mixed Oxides ( $\text{MO}_x$ ) configuration. 1 and 2 indicates fuel assemblies with 2.1% and 3.2%  $\text{U}_{235}$  enrichment respectively, 2 is  $\text{MO}_x$ , 3 is the stainless reflector while 4 is the external borated water.

mentioned in section 2, the cell calculation allows to consider each assembly as homogeneous, therefore each perturbation affecting the assembly has to be considered in the cell meta-model.

Following the benchmark specifications for the PWR-like cells, the fuel assemblies can be subjected to physical perturbations related to the fuel fabrication process. These physical uncertainties, listed in the following, affect only the fuel pins composing the assemblies, depicted in Figure 2, and are assumed to vary in a range  $[\mu - 3\sigma, \mu + 3\sigma]$ , where  $\mu$  and  $\sigma$  are the mean and the standard deviation of the each parameter, respectively:

- fuel pellet density,  
 $\rho_p = 10.0681 \pm 0.17 \text{ kg/m}^3$
- fuel pellet diameter,  
 $D_p = 0.8253 \pm 0.0013 \text{ mm}$
- cladding thickness,  
 $t_c = 0.0617 \pm 0.025 \text{ mm}$
- fuel pellet  $\text{U}_{235}$  enrichment,  
 $e_p = 2.1 \pm 0.00224 \text{ w/o.}$

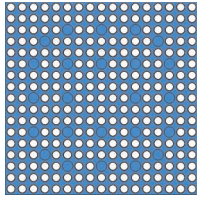


Fig. 2.: 2D representation of the 2.1% Uranium Oxides (UO<sub>x</sub>) assembly over which the two-group constant are homogenised during the cell calculation.

#### 4.1.1. Cell model tuning

In order to train the cell model, an approximation level of 2 has been chosen at first for the generation of the Smolyak sparse grid for the four parameters. However, due to the large *a posteriori* interpolation error, we have incremented the approximation order to 3, moving from 41 points to 137. It is interesting to notice that the third level Smolyak grid contains more points than the full tensor product  $3^q = 81$ , with  $q = 4$ . The training point set built with Smolyak algorithm allows us to reach a fill distance  $d$  approximately equal to  $1.7 \cdot 10^{-6}$ . Concerning the function  $f$  choice, two popular kinds of RBF have been investigated, the Inverse Multi Quadric (IMQ) and the Gaussian, respectively

$$f_{\text{IMQ},i}(\vec{p}) = \frac{1}{\sqrt{\|\vec{p} - \vec{p}_i\|^2 + \eta^2}} \quad (11)$$

$$f_{\text{G},i}(\vec{p}) = \exp\left(-\frac{\|\vec{p} - \vec{p}_i\|^2}{\eta^2}\right), \quad (12)$$

where  $\eta$  is the RBF shape parameter. Tables 1-2 show a sensitivity study performed in order to tune the RBF shape for the two cases under examination. As it can be noticed, even if the norm is slightly larger than  $d$ , the relative error between the full order Monte Carlo output  $\vec{x}$  and the cell NIROM result  $\vec{x}_u$  is acceptable for a shape factor of  $1 \cdot 10^{-4}$ . The output solution required  $\vec{x}$  contains the two-group data needed in equation (1), i.e.  $[D_1, D_2, \nu_1, \nu_2, \Sigma_{f,1}, \Sigma_{f,2}, \Sigma_{r,1}, \Sigma_{r,2}, \Sigma_{s,1 \rightarrow 2}]$ . The computational time required per each Monte Carlo run is approximately about 60 minutes with 30 CPUs on a Dell Precision Tower 7910 (Intel(R) Xeon(R) CPU E5-2630 v3 @ 2.40 GHz), while the time required by the NIROM Python module is slightly more than 1 second.

As expected, Tables 1-2 show that, when the untrained parameter is far from the training set, there is no shape factor able to acceptably approximate the full order solution. Both the examined cases show that the radial basis function choice

seems to have a little or even negligible impact on the results quality.

As regards the diffusion model, a uniform random sampling approach has been selected, due to the spatial nature of the perturbation. In particular, only five type 1 assemblies (please refer to Figure 1) have been perturbed per training point with the same perturbation intensity (an increase of 5% of the fission cross section with respect to the reference condition) in order to keep fixed the input dimension. The resulting set of 200 training solutions reached so far, however, seems still not enough in order to correctly reproduce the untrained configurations, since the filling distance still amounts to  $1.3 \cdot 10^2$ . This value is very large, especially if compared to the filling distance of the other meta-model, but seems also reasonable due to the extremely large number of possible combinations of perturbed assemblies (the combinations of 5 assemblies out of 170 is around  $10^9$ ).

## 5. Conclusions and future work

A two-step parametrised non-intrusive reduced order model for limiting the computational burden associated to core monitoring calculations has been proposed. The preliminary results highlighted the good capabilities of the cell model to reproduce the Monte Carlo calculation with an astonishing computational gain. Nevertheless, the model still requires a finer tuning, in order to try to reduce as much as possible the error with respect to the full order model, especially in the perspective of a coupling with the diffusion model. Moreover, it would be interesting to make use of an anisotropic Smolyak grid in order to better refine the parameter space in the most significant directions, after a proper sensitivity study. Regarding the diffusion model, future work will be carried out in order to increase the number of training configuration, exploiting smarter sampling strategies that could take into account also the presence of symmetry by rotation of the different core layout.

## Acknowledgement

Computational resources were provided by HPC at PoliTo, a project of Academic Computing within the Department of Control and Computer Engineering at the Politecnico di Torino. The Authors wish also to thank the colleague Dr. Antonio Froio for providing fundamental help with an *ad hoc* installation of FreeFEM++ on the department machines.

## References

- Abrate, N., Dulla, S., Ravetto, P., and Bruna, G. (2019). Convergence limits in perturbation theory. *International Conference on Mathematics and Computational Methods Applied to*

Table 1.: **The minimum distance between the untrained point and the training set,  $\min(\|\vec{p}_u - \vec{p}_i\|) = 7.3 \cdot 10^{-6}$ , is slightly larger than the fill distance  $d$  of the training set.**

|                         |                   |                   |                   |                   |
|-------------------------|-------------------|-------------------|-------------------|-------------------|
| Gaussian<br>shape fact. | $1 \cdot 10^0$    | $1 \cdot 10^{-1}$ | $1 \cdot 10^{-4}$ | $1 \cdot 10^{-6}$ |
| $\text{cond}(\hat{F})$  | $1 \cdot 10^{23}$ | $1 \cdot 10^{19}$ | $1 \cdot 10^{12}$ | $1 \cdot 10^0$    |
| $\ x_u - x\ /\ x\ $     | $7 \cdot 10^8$    | $2 \cdot 10^8$    | $5 \cdot 10^{-3}$ | $6 \cdot 10^{-1}$ |

Table 2.: **The minimum distance between the untrained point and the training set,  $\min(\|\vec{p}_u - \vec{p}_i\|) = 7.3 \cdot 10^{-6}$ , is slightly larger than the fill distance  $d$  of the training set.**

|                        |                |                   |                   |                   |
|------------------------|----------------|-------------------|-------------------|-------------------|
| IMQ<br>shape fact.     | $1 \cdot 10^0$ | $1 \cdot 10^{-1}$ | $1 \cdot 10^{-4}$ | $1 \cdot 10^{-6}$ |
| $\text{cond}(\hat{F})$ | $5 \cdot 10^5$ | $2 \cdot 10^6$    | $4 \cdot 10^{11}$ | $5 \cdot 10^7$    |
| $\ x_u - x\ /\ x\ $    | $7 \cdot 10^8$ | $3 \cdot 10^7$    | $5 \cdot 10^{-3}$ | $6 \cdot 10^{-1}$ |

Table 3.: **The minimum distance between the untrained point and the training set,  $\min(\|\vec{p}_u - \vec{p}_i\|) = 10^{-4}$ , is two orders of magnitude larger than the fill distance  $d$  of the training set.**

|                         |                |                   |                   |                   |
|-------------------------|----------------|-------------------|-------------------|-------------------|
| Gaussian<br>shape fact. | $1 \cdot 10^0$ | $1 \cdot 10^{-1}$ | $1 \cdot 10^{-4}$ | $1 \cdot 10^{-6}$ |
| $\text{cond}(\hat{F})$  | $1 \cdot 10^5$ | $3 \cdot 10^7$    | $3 \cdot 10^{15}$ | $6 \cdot 10^7$    |
| $\ x_u - x\ /\ x\ $     | $2 \cdot 10^9$ | $1 \cdot 10^{12}$ | $1 \cdot 10^0$    | $1 \cdot 10^0$    |

Table 4.: **The minimum distance between the untrained point and the training set,  $\min(\|\vec{p}_u - \vec{p}_i\|) = 10^{-4}$ , is two orders of magnitude larger than the fill distance  $d$  of the training set.**

|                        |                |                   |                   |                   |
|------------------------|----------------|-------------------|-------------------|-------------------|
| IMQ<br>shape fact.     | $1 \cdot 10^0$ | $1 \cdot 10^{-1}$ | $1 \cdot 10^{-4}$ | $1 \cdot 10^{-6}$ |
| $\text{cond}(\hat{F})$ | $5 \cdot 10^5$ | $2 \cdot 10^6$    | $4 \cdot 10^{11}$ | $5 \cdot 10^7$    |
| $\ x_u - x\ /\ x\ $    | $7 \cdot 10^8$ | $5 \cdot 10^7$    | $4 \cdot 10^1$    | $9 \cdot 10^{-1}$ |

*Nuclear Science and Engineering (M&C 2019)*, (3):2381–2390.

Gandini, A. (1987). Generalized Perturbation Theory (GPT) Methods. A Heuristic Approach. In Lewins J. and Becker M., editors, *Advances in Nuclear Science and Technology. Advances in Nuclear Science and Technology, vol 19*. Springer, Boston.

Hecht, F. (2012). New development in FreeFem++. *J. Numer. Math.*, 20(3-4):251–265.

Henry, A. F. (1975). *Nuclear Reactor Analysis Cambridge*. MIT Press, Massachusetts.

Ivanov, K. N., Avramova, M., Kamerow, S., Kodeli, I., Sartori, E., Ivanov, E., and Cabellos, O. (2013). Analysis in Modelling (UAM) for the Design, Operation and Safety Analysis of LWRs. Volume I : Specification and Benchmark for Uncertainty. I(May).

Judd, K. L., Maliar, L., Maliar, S., and Valero, R. (2014). Smolyak method for solving dynamic economic models: Lagrange interpolation, anisotropic grid and adaptive domain. *Journal of Economic Dynamics and Control*, 44:92–123.

Leppänen, J., Pusa, M., Viitanen, T., Valtavirta, V., and Kaltiaisenaho, T. (2015). The Serpent Monte Carlo code: Status, development and applications in 2013. *Annals of Nuclear Energy*, 82:142–150.

Rogers, C. A., Kassab, A. J., Divo, E. A., Ostrowski, Z., and Bialecki, R. A. (2012). An inverse POD-RBF network approach to parameter estimation in mechanics. *Inverse Problems in Science and Engineering*, 20(5):749–767.

Sargeni, A., Burn, K. W., and Bruna, G. B. (2016). The impact of heavy reflectors on power distribution perturbations in large PWR reactor cores. *Annals of Nuclear Energy*, 94:566–575.

Schaback, R. (1995). Error estimates and condition numbers for radial basis function interpola-

- tion. *Advances in Computational Mathematics*, 3(3):251–264.
- Smolyak, S. A. (1963). Quadrature and interpolation formulas for tensor products of certain classes of functions. *Dokl. Akad. Nauk SSSR*, 148(5):1042–1045.
- Sullivan, T. J. (2015). *Introduction to Uncertainty Quantification*, volume 63. Springer.
- Volkwein, S. (2013). Proper orthogonal decomposition: Theory and reduced-order modelling. *Lecture Notes, University of Konstanz*, 4:4.
- Wigner, E. P. and Weinberg, A. M. (1958). *The Physical Theory of Neutron Chain Reactors*.
- Xiao, D., Fang, F., Pain, C. C., and Navon, I. M. (2017). A parameterized non-intrusive reduced order model and error analysis for general time-dependent nonlinear partial differential equations and its applications. *Computer Methods in Applied Mechanics and Engineering*, 317:868–889.